Correlated noise and critical dimensions

Harukuni Ikeda *
Department of Physics, Gakushuin University, 1-5-1 Mejiro, Toshima-ku, Tokyo 171-8588, Japan

(Received 6 April 2023; revised 3 August 2023; accepted 15 November 2023; published 13 December 2023)

In equilibrium, the Mermin-Wagner theorem prohibits the continuous symmetry breaking for all dimensions $d \leqslant 2$. In this work, we discuss that this limitation can be circumvented in nonequilibrium systems driven by the spatiotemporally long-range anticorrelated noise. We first compute the lower and upper critical dimensions of the O(n) model driven by the spatiotemporally correlated noise by means of the dimensional analysis. Next we consider the spherical model, which corresponds to the large-n limit of the O(n) model and allows us to compute the critical dimensions and critical exponents, analytically. Both results suggest that the critical dimensions increase when the noise is positively correlated in space and time and decrease when anticorrelated. We also report that the spherical model with the correlated noise shows the hyperuniformity and giant number fluctuation even well above the critical point.

DOI: 10.1103/PhysRevE.108.064119

I. INTRODUCTION

The minimum dimension required for a phase transition to occur is known as the lower critical dimension d_l [1]. For systems with quenched randomness, Imry and Ma predicted that the lower critical dimension is $d_l = 2$ for a discrete order parameter and $d_l = 4$ for a continuous order parameter [2]. Recent studies have reported that d_l can be reduced by introducing anticorrelation to the quenched randomness. For example, in Ref. [3], the authors studied the random field Ising model with the anticorrelated random field and showed that the ordered phase arises on the ground state even in $d = 2$. Reference [4] reported a first-order transition of the Potts model on a random Voronoi lattice in $d = 2$. The authors in Ref. [5] argued that this is a consequence of the strong anticorrelation in the coordination number of the random Voronoi lattices, which reduces the lower critical dimension. Similar anticorrelation also appears in the Ising model in the aperiodic field, which stabilizes the ferromagnetic ground state even in $d = 1$ [6,7].

For equilibrium systems without quenched randomness, the Mermin-Wagner theorem claims that the lower-critical dimension of the continuous symmetry breaking is $d_l = 2$ [8]. However, for out-of-equilibrium systems, the continuous symmetry breaking can occur even $d \leqslant 2$; some examples include the XY model driven by anisotropic noise [9,10], the O(n) model driven by shear [11,12], Vicsek model [13,14], and so on [15,16]. A recent numerical study suggests that so-called hyperuniform states of matter [17] may potentially be added to the list above [18]. The hyperuniform states of matter are characterized by the anomalous suppression of the density fluctuation on a large scale, which leads to the vanishing of the static structure factor $S(q)$ in the limit of the small wave number $\lim_{q\to} S(q) = 0$ [17]. This property is referred to as the hyperuniformity (HU), which was first introduced for density fluctuation but later has been extended to fluctuations of more general quantities, such as spin variables and vector fields [17]. In Ref. [18], Galliano *et al.* proposed and numerically demonstrated that the suppression of the density fluctuation also reduces d_l, leading to the perfect crystalline phase even in $d = 2$.

The HU is widely observed in various systems such as Vycor glass [19], periodically driven emulsions [20], chiral active matter [21,22], and so on [17]. While no unified theory has been found that can comprehensively explain the HU observed in all these systems, if it exists, Hexner and Levine proposed that the HU can universally appear for systems having certain symmetries [23]. In Ref. [23], they derived a Langevin equation for a system conserving the total number of particles and center of mass. The effective noise of the resultant Langevin equation has spatial anticorrelation, which leads to the HU [23,24]. Other examples showing the HU are chiral active matter [21,22], where the periodic nature of the driving force leads to the temporal anticorrelation of the effective noise, which results in the HU [25,26]. These results suggest that spatial or temporal anticorrelation of the noise leads to HU, which may reduce d_l.

Based on the above observations, it is tempting to conjecture that the anticorrelation of the noise or quenched randomness generally reduces the lower critical dimension. Our first goal is to test this conjecture. The second goal is to investigate the effects of the long-range temporal correlation of the noise on critical phenomena. The effects of the temporally correlated noise on a single particle have been investigated significantly in the context of anomalous diffusion [27,28]. However, its effects on many-body systems, in particular near the critical point, have not been investigated sufficiently before. For those goals, here we investigate the effects of the spatiotemporally correlated noise on the second-order phase transition by using the O(n) and spherical models. As discussed in the following paragraph, the noise encom-

*harukuni.ikeda@gakushuin.ac.jp

passes the time-independent random field and equilibrium white noise in certain limits.

For concreteness, we consider model-A and -B dynamics [1,29] with the correlated noise $\xi(\boldsymbol{x},t)$ of zero mean and variance

$$\langle \xi(\boldsymbol{x},t)\xi(\boldsymbol{x}',t')\rangle = 2TD(\boldsymbol{x}-\boldsymbol{x}',t-t'), \tag{1}$$

where $D(\boldsymbol{x},t)$ represents the spatiotemporal correlation of the noise. The Fourier transform of $D(\boldsymbol{x},t)$ w.r.t. $\boldsymbol{x}$ and t is given by

$$D(\boldsymbol{q},\omega) = |\boldsymbol{q}|^{-2\rho}|\omega|^{-2\theta}, \tag{2}$$

where $\boldsymbol{q}$ denotes the wave vector and ω denotes the frequency. The same correlation function has been considered in previous works to investigate the effects of the long-range spatiotemporal correlation on the Kardar-Parisi-Zhang (KPZ) equation [30–33]. When $\rho=\theta=0$, the noise can be identified with the white noise in equilibrium. The positive values of ρ and θ represent the positive power-law correlation in the real space: $D(\boldsymbol{x},t)\sim|\boldsymbol{x}|^{2\rho-d}|t|^{2\theta-1}$, where d denotes the spatial dimension. In the limit $\theta\to 1/2$, the noise correlation does not decay with time, and thus the noise can be identified with the quenched random field. The negative values of ρ and θ imply the existence of the anticorrelation because $D(\boldsymbol{q}=0,\omega=0)=\int d\boldsymbol{x}\int dt D(\boldsymbol{x},t)=0$. Therefore, the model can smoothly connect the white noise ($\rho=\theta=0$), quenched randomness ($\theta\to 1/2$), positively correlated noise ($\theta>0$, $\rho>0$), and anticorrelated noise ($\theta<0$, $\rho<0$) by changing ρ and θ. In this work, we show that the positive correlation increases the lower and upper critical dimensions d_l and d_u, and the anticorrelation reduces d_l and d_u.

The structure of the paper is as follows. In Sec. II, we investigate the O(n) model driven by the model-A dynamics with the correlated noise by means of the dimensional analysis. Section III, we investigate the spherical model, which corresponds to the $n\to\infty$ limit of the O(n) model and allows us to calculate the critical dimensions analytically [1]. We also discuss that the positive correlation of the noise induces the giant number fluctuation (GNF), i.e., the anomalous enhancement of the fluctuation even far above the critical point. On the contrary, the anticorrelation of the noise suppresses the fluctuation and induces the HU. In Sec. IV, we discuss the behavior of the conserved order parameter driven by the model-B dynamics with the correlated noise. In Sec. V, we summarize the work.

II. DIMENSIONAL ANALYSIS

Here we derive the upper and lower critical dimensions of the O(n) model driven by the model-A dynamics with the correlated noise.

A. Model

Let $\vec{\phi}=\{\phi_1,\dots,\phi_n\}$ be a nonconserved n-component order parameter. We assume that the time evolution of $\phi_a(\boldsymbol{x},t)$ follows the model-A dynamics [29]:

$$\frac{\partial\phi_a(\boldsymbol{x},t)}{\partial t} = -\Gamma\frac{\delta F[\vec{\phi}]}{\delta\phi_a(\boldsymbol{x},t)} + \xi_a(\boldsymbol{x},t), \tag{3}$$

where Γ denotes the damping coefficient and ξ_a denotes the noise. $F[\vec{\phi}]$ denotes the free energy of the O(n) model [1]:

$$F[\vec{\phi}] = \int d\boldsymbol{x}\left[\frac{\sum_{a=1}^n\nabla\phi_a\cdot\nabla\phi_a}{2}+\frac{\varepsilon|\vec{\phi}|^2}{2}+\frac{g|\vec{\phi}|^4}{4}\right], \tag{4}$$

where $|\vec{\phi}|^2=\sum_{a=1}^n\phi_a^2$, ε denotes the linear distance to the transition point, and g denotes the strength of the nonlinear term. The mean and variance of the noise $\xi_a(\boldsymbol{x},t)$ are

$$\begin{aligned}&\langle\xi_a(\boldsymbol{x},t)\rangle = 0,\\ &\langle\xi_a(\boldsymbol{x},t)\xi_b(\boldsymbol{x}',t')\rangle = 2T\delta_{ab}\Gamma D(\boldsymbol{x}-\boldsymbol{x}',t-t'),\end{aligned} \tag{5}$$

where $D(\boldsymbol{x},t)$ represents the correlation of the noise. We assume that the correlation in the Fourier space is written as [30–33]

$$D(\boldsymbol{q},\omega) = |\boldsymbol{q}|^{-2\rho}|\omega|^{-2\theta}. \tag{6}$$

To ensure the existence of the Fourier transform of $D(\boldsymbol{q},\omega)$, the values of ρ and θ are constrained to $\rho<d/2$ and $\theta<1/2$, and one should introduce the high-frequency cutoff for $\theta\leqslant -1/2$. The noise can be generated, for instance, by integrating uncorrelated white noise $\eta_a(\boldsymbol{x},t)$ with a proper kernel $K(\boldsymbol{x},t)$:

$$\xi_a(\boldsymbol{x},t) = \int_{-\infty}^{\infty}dt\int d\boldsymbol{x}K(\boldsymbol{x}-\boldsymbol{x}',t-t')\eta_a(\boldsymbol{x}',t'), \tag{7}$$

where $K(\boldsymbol{x},t)$ satisfies $K(\boldsymbol{x},t)=0$ for $t<0$ and $|K(\boldsymbol{q},\omega)|\sim|\boldsymbol{q}|^{-\rho}|\omega|^{-\theta}$ in the Fourier space [30]. Another way to generate the correlated noise would be to perturb periodic patterns, which naturally leads to the anticorrelation ($\rho<0$ and $\theta<0$) [34], see also Sec. V D for a related discussion. The model satisfies the fluctuation-dissipation theorem only when $\rho=\theta=0$ [35]. For $\rho\neq 0$ or $\theta\neq 0$, on the contrary, the model violates the detailed balance, and thus the steady-state distribution is not given by the Maxwell-Boltzmann distribution [36].

B. Critical dimensions

From Eqs. (3) and (4), we get

$$\dot{\phi}_a = -\Gamma(-\nabla^2\phi_a+\varepsilon\phi_a+g\phi_a|\vec{\phi}|^2)+\xi_a, \tag{8}$$

Now we consider the following scaling transformations: $x\to bx$, $t\to b^{z_t}t$, $\phi_a\to b^{z_\phi}\phi_a$, and $g\to b^{z_g}g$ [1]. To calculate the scaling dimension of the noise, we observe the fluctuation induced by the noise in a $(d+1)$-dimensional Euclidean space $[0,l]^d\times[0,t]$ [17]:

$$\sigma(l,t)^2 \equiv \left\langle\left(\int_{\boldsymbol{x}'\in[0,l]^d}d\boldsymbol{x}'\int_0^t dt'\xi_a(\boldsymbol{x}',t')\right)^2\right\rangle. \tag{9}$$

The asymptotic behavior for $l\gg 1$ and $t\gg 1$ is

$$\sigma(l,t)^2 \sim (c_1t^{1+2\theta}+c_2t^0)(c_3l^{d+2\rho}+c_4l^{d-1}), \tag{10}$$

where c_i denotes a constant and c_2t^0, c_4l^{d-1} account for the surface contributions [17,37]. Equation (10) implies $\xi(\boldsymbol{x},t)\to b^{z_t(2\theta'-1)/2}b^{(2\rho'-d)/2}\xi(\boldsymbol{x},t)$, where

$$\rho' = \max[\rho,-1/2],\ \theta' = \max[\theta,-1/2]. \tag{11}$$

Assuming the scaling invariance of the dynamics Eq. (8), we get [1,38]

$$z_t = 2, \quad z_g = -2z_\phi - z_t, \quad z_\phi = 1 + \frac{2\rho' - d}{2} + 2\theta'. \tag{12}$$

The simplest way to calculate the lower critical dimension d_l is to observe the fluctuation of the order parameter:

$$\langle \delta\phi_a^2 \rangle \sim b^{2z_\phi}. \tag{13}$$

To ensure the stability of the ordered phase, z_ϕ must be negative; otherwise, the fluctuation of the order parameter diverges in the thermodynamic limit $b \to \infty$, which destroys the long-range order. Therefore, the lower-critical dimension can be determined by setting $z_\phi = 0$, leading to

$$d_l = 2 + 2\rho' + 4\theta'. \tag{14}$$

Equation (12) implies that the coupling of the nonlinear term g scales as $g' = b^{-z_g} g$ under the scaling transformation $x' = b^{-1}x$ [1,38]. When $z_g > 0$, the nonlinear term is irrelevant and vice versa. Therefore, the upper critical dimension is obtained by setting $z_g = 0$, leading to

$$d_u = 4 + 2\rho' + 4\theta'. \tag{15}$$

When $\rho = \theta = 0$, we get $d_l = 2$ and $d_u = 4$, which are consistent with the standard O(n) model in equilibrium [1]. When $\rho \neq 0$ or $\theta \neq 0$ on the contrary, the system reaches the nonequilibrium steady state because the noise does not satisfy the detailed balance. In this case, the positive correlation of the noise ($\rho > 0$, $\theta > 0$) increases the critical dimensions, d_l and d_u, and the anticorrelation reduces d_l and d_u.

C. Correlated random field

In the limit $\theta \to 1/2$, the noise correlation does not decay with time $D(\boldsymbol{x}, t) \sim t^{2\theta-1} \to t^0$, and thus the noise can be identified with the correlated random field. In this case, we get

$$d_l^{\mathrm{RF}} = 4 + 2\rho'. \tag{16}$$

It would be instructive to compare the above result with the standard Imry-Ma argument for the lower critical dimension [2,3,37]. In a domain of linear size l, the typical fluctuation induced by the correlated random field is $\sigma^2 \equiv \langle (\int_{\boldsymbol{x}\in[0,l]^d} d\boldsymbol{x} h)^2 \rangle \sim c_1 l^{d+2\rho} + c_2 l^{d-1}$ [3,37]. The domain wall energy is $\gamma \sim l^{d-1}$ for a discrete order parameter and $\gamma \sim l^{d-2}$ for a continuous order parameter [2]. When $\sigma \gg \gamma$, the fluctuation of the random field destroys the ordered phase and vice versa. Therefore, on the lower critical dimension d_l, $\sigma \sim \gamma$, leading to [3]

$$d_l^{\mathrm{I.M.}} = \begin{cases} 2 + 2\rho' & \text{(discrete)}, \\ 4 + 2\rho' & \text{(continuous)}. \end{cases} \tag{17}$$

The result for a continuous order parameter is consistent with that of the dimensional analysis Eq. (16).

III. SPHERICAL MODEL

Due to the nonlinear term in the free-energy Eq. (4), the O(n) model cannot be solved analytically. Here we instead consider a solvable model: the spherical model, which corresponds to the $n \to \infty$ limit of the O(n) model [1,39].

A. Model

The effective free energy of the model is

$$F[\phi] = \int d\boldsymbol{x} \left[\frac{(\nabla\phi)^2}{2} + \frac{\mu\phi^2}{2} \right], \tag{18}$$

where μ denotes the Lagrange multiplier to impose the spherical constraint [40]:

$$\int d\boldsymbol{x} \langle \phi(\boldsymbol{x})^2 \rangle = N. \tag{19}$$

We impose the spherical constraint for the mean value. One can, in principle, consider a rigid constraint $\int d\boldsymbol{x}\phi(\boldsymbol{x})^2 = N$, instead of Eq. (19). The dynamics with the rigid constraint has some nonlinear terms that make the model difficult to solve analytically. This paper only consider the constraint for the mean-value Eq. (19).

For $\rho = \theta = 0$, the steady-state distribution is given by the Boltzmann distribution, and thus one does not need to solve the dynamical equation. In this case, the two-point correlation of the spherical model with the constraint Eq. (19) agrees with that of the rigid constraint above the critical temperature T_c but is inconsistent below T_c [41]. So hereafter we only focus on the behavior above T_c.

B. Steady-state solution

By substituting Eq. (18) into Eq. (3) we get a linear differential equation:

$$\dot{\phi} = -\Gamma(-\nabla^2\phi + \mu\phi) + \xi. \tag{20}$$

This can be easily solved in the Fourier space,

$$\phi(\boldsymbol{q}, \omega) = \frac{\xi(\boldsymbol{q}, \omega)}{i\omega + \Gamma(q^2 + \mu)}, \tag{21}$$

where

$$\mathcal{O}(\boldsymbol{q}, \omega) = \int dt \int d\boldsymbol{x} e^{-i\boldsymbol{q}\cdot\boldsymbol{x} - i\omega t} \mathcal{O}(\boldsymbol{x}, t). \tag{22}$$

The two-point correlation is calculated as

$$\langle \phi(\boldsymbol{q}, \omega)\phi(\boldsymbol{q}', \omega') \rangle = (2\pi)^{d+1}\delta(\boldsymbol{q} + \boldsymbol{q}')\delta(\omega + \omega')S(q, \omega), \tag{23}$$

where

$$S(q, \omega) \equiv \int dt \int d\boldsymbol{x} e^{i\boldsymbol{q}\cdot\boldsymbol{x} + i\omega t} \langle \phi(\boldsymbol{x}, t)\phi(0, 0) \rangle = \frac{2T\Gamma D(\boldsymbol{q}, \omega)}{\omega^2 + \Gamma^2(kq^2 + \mu)^2}. \tag{24}$$

C. Correlation length and relaxation time

Since we are interested in the critical behaviors in large spatiotemporal scales, here we analyze the scaling behavior of the correlation function for $|\boldsymbol{q}| \ll 1$ and $\omega \ll 1$. After some manipulations, we get

$$S(q, \omega) = T\mu^{-2-\rho-2\theta} \mathcal{S}(\mu^{-1/2}q, \mu^{-1}\omega), \tag{25}$$

where

$$\mathcal{S}(x, y) = \frac{2\Gamma x^{-2\rho} y^{-2\theta}}{y^2 + \Gamma^2 (x^2 + 1)^2}. \tag{26}$$

The scaling Eq. (25) implies that the correlation length ξ and relaxation time τ behave as

$$\xi \sim \mu^{-1/2}, \ \tau \sim \xi^z, \tag{27}$$

with the dynamic critical exponent

$$z = 2. \tag{28}$$

The correlation length and relaxation time diverge in the limit $\mu \to 0$, meaning that $\mu = 0$ defines the critical point.

D. Static structure factor

The static structure factor $S(\boldsymbol{q})$ is calculated as

$$S(\boldsymbol{q}) = \frac{1}{2\pi} \int_{-\infty}^{\infty} d\omega S(\boldsymbol{q}, \omega) = \frac{AT q^{-2\rho}}{(q^2 + \mu)^{1+2\theta}}, \tag{29}$$

where

$$A = \frac{1}{\pi} \int_{-\infty}^{\infty} \frac{|x|^{-2\theta} dx}{x^2 + 1} = \sec(\pi\theta). \tag{30}$$

Note that this integral diverges when $\theta \geqslant 1/2$ or $\theta \leqslant -1/2$. So hereafter we only discuss the behaviors for $-1/2 < \theta < 1/2$ so that A remains finite. $S(q)$ shows the power-law behavior for $q \ll \mu^{1/2} \approx \xi^{-1}$:

$$S(q) \sim q^{-2\rho}. \tag{31}$$

For $\rho > 0$, $S(q) \to \infty$ for small q, leading to the power-law correlation

$$G(\boldsymbol{x}) = \langle \phi(\boldsymbol{x}) \phi(0) \rangle \sim |\boldsymbol{x}|^{2\rho - d}. \tag{32}$$

As a consequence, the fluctuation of the order parameter in the d-dimensional square box $[0, l]^d$ behaves as [17]

$$\sigma(l)^2 \equiv \left\langle \left(\int_{\boldsymbol{x} \in [0,l]^d} d\boldsymbol{x} \phi(\boldsymbol{x}) \right)^2 \right\rangle \sim l^{d+2\rho}, \tag{33}$$

which is much larger than the naive expectation from the central limit theorem $\sigma^2 \sim l^d$. This anomalous enhancement of the fluctuation is the signature of the GNF [42]. For $\rho < 0$, $S(q) \to 0$ in the limit $q \to 0$. In this case, the fluctuation of the order parameter Eq. (33) is highly suppressed, i.e., the model exhibits the HU [17]. To visualize these results, we show typical behaviors of $S(q)$ in Fig. 1.

E. Lagrange multiplier

The remaining task is to determine the Lagrange multiplier μ by the spherical constraint:

$$N = \int d\boldsymbol{x} \langle \phi(\boldsymbol{x}, t)^2 \rangle = \frac{V}{(2\pi)^d} \int d\boldsymbol{q} S(q), \tag{34}$$

where $V = \int d\boldsymbol{x}$ denotes the volume of the system. Substituting Eq. (29) into Eq. (34), we get

$$1 = TA' \int_0^{q_D} dq \frac{q^{d-1-2\rho}}{(q^2 + \mu)^{1+2\theta}}, \tag{35}$$

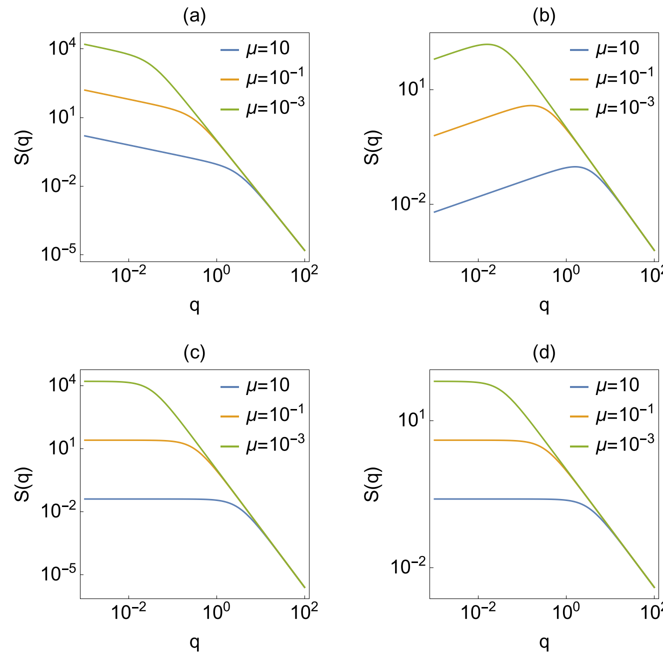

FIG. 1. Typical behaviors of $S(q)$ of spherical model for model A: (a) $S(q)$ for positive spatial correlation ($\rho = 0.2, \theta = 0$). $S(q)$ diverges in the limit of small q even far from the transition point, i.e., the GNF appears. (b) $S(q)$ for negative spatial correlation ($\rho = -0.2, \theta = 0$). $S(q)$ vanishes in the limit of small q, i.e., the HU appears. (c) $S(q)$ for positive temporal correlation ($\rho = 0, \theta = 0.2$). (d) $S(q)$ for negative temporal correlation ($\rho = 0, \theta = -0.2$). The temporal correlation alone cannot induce the GNF or HU. For simplicity, here we set $A = T = 1$.

where q_D denotes the cutoff and

$$A' = \frac{\Omega_d A}{(2\pi)^d} \frac{V}{N}. \tag{36}$$

Here Ω_d denotes the d-dimensional solid angle. Substituting $\mu = 0$ into Eq. (35), one can calculate the critical temperature T_c as follows:

$$T_c = \begin{cases} 0 & d \leqslant d_l \\ (d - d_l)/A' q_D^{d-d_l} & d > d_l \end{cases}, \tag{37}$$

where we have defined the lower critical dimension as

$$d_l = 2 + 2\rho + 4\theta, \ (-1/2 < \theta < 1/2). \tag{38}$$

This is consistent with the result of the dimensional analysis Eq. (14) for $\rho > -1/2$. On the contrary, the results are inconsistent for $\rho < -1/2$. Further studies would be beneficial to elucidate this point, but anyway, the qualitative result remains the same: The positive correlation increases d_l, and the anti-correlation reduces d_l.

The detailed analysis of Eq. (35) near T_c leads to (see Appendix A)

$$\mu \sim (T - T_c)^\gamma \tag{39}$$

with

$$\gamma = \begin{cases} \frac{2}{d - d_l} & d_l < d < d_u \\ 1 & d > d_u, \end{cases}, \tag{40}$$

where the upper critical dimension d_u is

$$d_u = 4 + 2\rho + 4\theta, (-1/2 < \theta < 1/2). \tag{41}$$

Again the result is consistent with the dimensional analysis for $\rho > -1/2$. Substituting this result into Eq. (27), we can determine the critical exponent:

$$\xi \sim (T - T_c)^{-\nu} \tag{42}$$

with

$$\nu = \begin{cases} 1/(d - d_l) & d_l < d < d_u \\ 1/2 & d > d_u \end{cases}. \tag{43}$$

The critical exponent differs from the equilibrium value if $2\rho + 4\theta \neq 0$ since $d_l \neq d_l^{\mathrm{eq}} = 2$. In other words, the long-range spatiotemporal correlation of the noise changes the universality class.

IV. CONSERVED ORDER PARAMETER

Let $\vec{\phi} = \{\phi_1, \dots, \phi_n\}$ be a conserved n-component order parameter. We assume that the time evolution of $\phi_a(\boldsymbol{x}, t)$ is described by the model-B dynamics [29],

$$\frac{\partial \phi_a(\boldsymbol{x}, t)}{\partial t} = \Gamma \nabla^2 \frac{\delta F[\vec{\phi}]}{\delta \phi_a(\boldsymbol{x}, t)} + \boldsymbol{\nabla} \cdot \boldsymbol{\xi}_a(\boldsymbol{x}, t), \tag{44}$$

where Γ denotes the damping coefficient, $\boldsymbol{\xi}_a = \{\xi_{a,\mu}\}_{\mu=1,\dots,d}$ denotes the noise, and d denotes the spatial dimension. The mean and variance of the noise $\xi_{a,\mu}(\boldsymbol{x}, t)$ are given by

$$\langle \xi_{a,\mu}(\boldsymbol{x}, t) \rangle = 0,$$
$$\langle \xi_{a,\mu}(\boldsymbol{x}, t) \xi_{b,\nu}(\boldsymbol{x}', t') \rangle = 2T \delta_{ab} \delta_{\mu\nu} \Gamma D(\boldsymbol{x} - \boldsymbol{x}', t - t'), \tag{45}$$

where the Fourier transform of $D(\boldsymbol{x}, t)$ is given by Eq. (6).

A. Dimensional analysis for O(n) model

Substituting the free energy Eq. (4) into Eq. (44), we get

$$\dot{\phi}_a = \Gamma \nabla^2 (-\nabla^2 \phi_a + \varepsilon \phi_a + g \phi_a |\vec{\phi}|^2) + \boldsymbol{\nabla} \cdot \boldsymbol{\xi}_a. \tag{46}$$

As before, we consider the scaling transformations: $x \to bx$, $t \to b^{z_t} t$, $\phi_a \to b^{z_\phi} \phi_a$, and $g \to b^{z_g} g$ [1]. Assuming the scaling invariance of the dynamic equation Eq. (46), we get

$$z_t = 4, \quad z_g = 2 - 2z_\phi - z_t, \quad z_\phi = 1 + \frac{2\rho' - d}{2} + 4\theta', \tag{47}$$

where $\rho' = \max[\rho, -1/2]$ and $\theta' = \max[\theta, -1/2]$, as defined in Eq. (11). As before, the lower critical dimension is calculated by setting $z_\phi = 0$, leading to

$$d_l = 2 + 2\rho' + 8\theta'. \tag{48}$$

The upper critical dimension is obtained by setting $z_g = 0$, leading to

$$d_u = 4 + 2\rho' + 8\theta'. \tag{49}$$

When $\theta = 0$, the results are consistent with those of the model A, see Sec. II, while when $\theta \neq 0$, we get different results. Aside from such a difference, the qualitative conclusion remains the same: The positive correlation of the noise ($\rho > 0$ and $\theta > 0$) increases the critical dimensions d_l and d_u, while the anticorrelation ($\rho < 0$ and $\theta < 0$) reduces d_l and d_u.

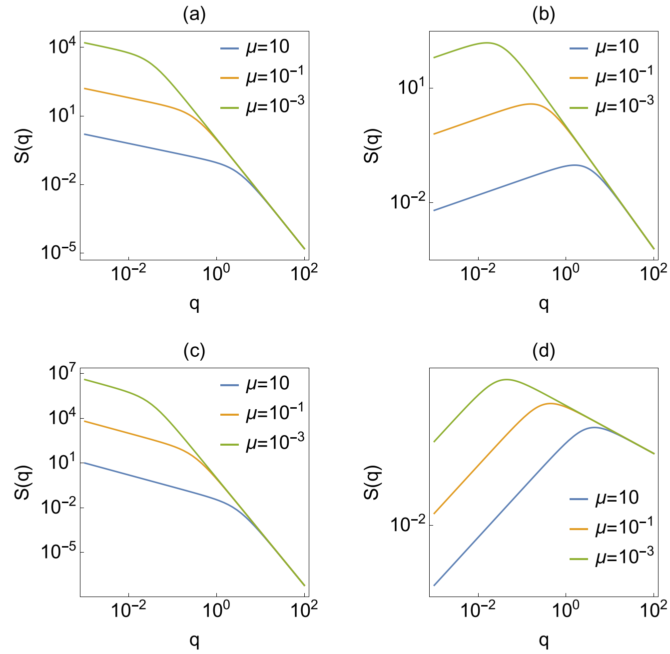

FIG. 2. Typical behaviors of $S(q)$ of spherical model for model B: (a) $S(q)$ for positive spatial correlation ($\rho = 0.2, \theta = 0$). (b) $S(q)$ for negative spatial correlation ($\rho = -0.2, \theta = 0$). (c) $S(q)$ for positive temporal correlation ($\rho = 0, \theta = 0.2$). (d) $S(q)$ for negative temporal correlation ($\rho = 0, \theta = -0.2$). For positive spatial or temporal correlation, $S(q)$ diverges in the limit of small q even far from the transition point, i.e., the GNF appears. For negative spatial or temporal correlation, on the contrary, $S(q)$ vanishes in the limit of small q, i.e., the HU appears. For simplicity, here we set $B = T = 1$.

B. Spherical model

The spherical model for the model-B dynamics is

$$\dot{\phi} = \Gamma \nabla^2 (-\nabla^2 \phi + \mu \phi) + \boldsymbol{\nabla} \cdot \boldsymbol{\xi}. \tag{50}$$

This model neglects the nonlinear term of the O(n) model and instead impose the spherical constraint $\int d\boldsymbol{x} \langle \phi^2 \rangle = N$. One can solve it easily since this is a linear equation. For instance, the static structure factor $S(\boldsymbol{q})$ in the steady state is calculated as

$$S(\boldsymbol{q}) = \frac{BT q^{-2\rho - 4\theta}}{(q^2 + \mu)^{1+2\theta}}, \tag{51}$$

where B denotes a constant,

$$B = \frac{1}{\Gamma^{2\theta} \pi} \int_{-\infty}^{\infty} \frac{|x|^{-2\theta} dx}{x^2 + 1} = \frac{\sec(\pi\theta)}{\Gamma^{2\theta}}. \tag{52}$$

As before, we restrict θ to $-1/2 < \theta < 1/2$ to keep B finite; $S(q)$ shows the power-law behavior for $q \ll \mu^{1/2} \approx \xi^{-1}$:

$$S(q) \sim q^{-2\rho - 4\theta}. \tag{53}$$

For $2\rho + 4\theta > 0$, $S(q) \to \infty$ for small q, leading to the GNF [42]. On the contrary, for $2\rho + 4\theta < 0$, $S(q) \to 0$ for small q, leading to the HU [17]. Interestingly, the GNF and HU appear even without the spatial correlation of the noise $\rho = 0$. To visualize the above results, we show typical behaviors of $S(q)$ in Fig. 2.

The Lagrange multiplier μ is to be determined by the spherical constraint $\int d\boldsymbol{x}\langle\phi^2\rangle = N$. As before, the detailed analysis of this equation allows us to calculate the lower and upper critical dimensions for $-1/2 < \theta < 1/2$ (see Appendix A),

$$d_l = 2 + 2\rho + 8\theta, \quad d_u = 4 + 2\rho + 8\theta. \tag{54}$$

For $\rho > -1/2$, the results are consistent with the dimensional analysis in the previous subsection. On the contrary, for $\rho < -1/2$, we get inconsistent results. Further studies would be beneficial to elucidate the origin of this discrepancy. Aside from such a minor difference, both O(n) and spherical models predict that the positive correlation of the noise ($\rho > 0$ and $\theta > 0$) increases the critical dimensions, d_l and d_u, while the anticorrelation reduces d_l and d_u.

For $d_l < d < d_u$ near T_c, the scaling behaviors of the Lagrange multiplier μ, correlation length ξ, and relaxation time τ are (see Appendix A)

$$\mu \sim (T - T_c)^\gamma, \quad \xi \sim (T - T_c)^\nu, \quad \tau \sim \xi^z, \tag{55}$$

where

$$\gamma = \frac{2}{d - d_l}, \quad \nu = \frac{1}{d - d_l}, \quad z = 4. \tag{56}$$

Note that the static critical exponent ν differs from the equilibrium values if $2\rho + 8\theta \neq 0$ because $d_l \neq d_l^{\rm eq} \equiv 2$ [1,40]. This implies that the long-range spatiotemporal correlation of the noise leads to a new universality class. Further theoretical and numerical studies would be beneficial to elucidate this point.

C. Center-of-mass conserving dynamics

An interesting application is for the systems driven by the center-of-mass conserving (COMC) dynamics, which was introduced to explain the HU [23,24]. The origin of the HU may depend on the detail of the system, but Hexner and Levine claimed that there is a universal mechanism to yield HU for systems conserving the center of mass [23]. Below we briefly summarize their argument for the model-B dynamics. Let $\rho(\boldsymbol{x}, t)$ be the density following the equation of continuity:

$$\frac{\partial\rho(\boldsymbol{x}, t)}{\partial t} = -\nabla\cdot\boldsymbol{J}(\boldsymbol{x}, \boldsymbol{t}), \tag{57}$$

where $\boldsymbol{J}$ denotes the flux. In the case of the standard model B, $\boldsymbol{J}$ is written as [43]

$$\boldsymbol{J} = -\Gamma\nabla\mu + \boldsymbol{\xi}, \tag{58}$$

where $\mu = \delta F/\delta\rho(\boldsymbol{x}, t)$ denotes the chemical potential and $\boldsymbol{\xi}$ denotes the noise. The conservation of the center of mass requires [23]

$$\begin{aligned}\frac{d\langle x_a\rangle}{dt} &= \int d\boldsymbol{x}x_a\frac{\partial\rho(\boldsymbol{x}, t)}{\partial t} = -\int d\boldsymbol{x}x_a\nabla\cdot\boldsymbol{J}(\boldsymbol{x}, t)\\ &= \int d\boldsymbol{x}J_a(\boldsymbol{x}, t) = \int d\boldsymbol{x}\xi_a = 0.\end{aligned} \tag{59}$$

To satisfy the last equality, ξ_a should be written in the form of a divergence of another vector:

$$\xi_a(\boldsymbol{x}, t) = \nabla\cdot\boldsymbol{\sigma}_a(\boldsymbol{x}, t) = \sum_b\frac{\partial\sigma_{ab}(\boldsymbol{x}, t)}{\partial x_b}. \tag{60}$$

TABLE I. Critical dimensions. Here we used abbreviations $\rho' = \max[-1/2, \rho]$ and $\theta' = \max[-1/2, \theta]$.

Model A	d_l	d_u
O(n) model	$2 + 2\rho' + 4\theta'$	$4 + 2\rho' + 4\theta'$
Spherical model ($-1/2 < \theta < 1/2$)	$2 + 2\rho + 4\theta$	$4 + 2\rho + 4\theta$
Model B	d_l	d_u
O(n) model	$2 + 2\rho' + 8\theta'$	$4 + 2\rho' + 8\theta'$
Spherical model ($-1/2 < \theta < 1/2$)	$2 + 2\rho + 8\theta$	$4 + 2\rho + 8\theta$

The simplest choice of $\sigma_{ab}(\boldsymbol{x}, t)$ is an isotropic white noise:

$$\langle\sigma_{ab}(\boldsymbol{x}, t)\sigma_{cd}(\boldsymbol{x}', t')\rangle \propto \delta_{ac}\delta_{bd}\delta(\boldsymbol{x} - \boldsymbol{x}')\delta(t - t'). \tag{61}$$

Then we get

$$\langle\xi_a(\boldsymbol{x}, t)\xi_b(\boldsymbol{x}', t')\rangle \propto \delta_{ab}\nabla^2\delta(\boldsymbol{x} - \boldsymbol{x}')\delta(t - t'), \tag{62}$$

which is tantamount to set $D(\boldsymbol{q}, \omega) \propto q^2$ in our model-B dynamics, i.e., $\rho = -1$ and $\theta = 0$; see Eq. (45). In this case, the static structure factor Eq. (53) behaves as $S(q) \sim q^2$ for a small waver number q. Therefore, the model exhibits the HU, as discussed in previous work [23]. Also, the dimensional analysis of the O(n) model and spherical model both predict that the lower critical dimension becomes lower than the equilibrium value, $d_l < d_l^{\rm eq} = 2$. This implies that the continuous symmetric breaking can occur even in $d = 2$ or lower dimension in contrast with the equilibrium systems for which the Mermin-Wagner theorem prohibits the long-range order. This appears to be consistent with a recent numerical simulation of a two-dimensional system driven by the COMC dynamics, where the authors reported the emergence of the perfect crystal phase even in $d = 2$ [18]. But strictly speaking, our model is for the second-order phase transition, and thus it cannot be directly applied to the first-order phase transition such as the crystaillization. Further numerical and theoretical studies would be beneficial.

V. SUMMARY AND DISCUSSIONS

A. Summary

In this work, we calculated the lower and upper critical dimensions, d_l and d_u, of the O(n) and spherical models driven by the model-A and -B dynamics with the correlated noise $\xi(\boldsymbol{x}, t)$, see Table I for a summary. The correlation of the noise is written in the Fourier space as $D(\boldsymbol{q}, \omega) = |\boldsymbol{q}|^{-2\rho}|\omega|^{-2\theta}$. Our results imply that the positive correlation of the noise ($\rho > 0$ and $\theta > 0$) increases the critical dimensions, d_l and d_u, while the anticorrelation ($\rho < 0$ and $\theta < 0$) reduces d_l and d_u. We also found that the static structure factor $S(q)$ in the paramagnetic phase exhibits the power-law behavior for small wave number $S(q) \sim q^\alpha$ with $\alpha = -2\rho$ for the nonconserved order parameter (model A) and $\alpha = -2\rho - 4\theta$ for the conserved order parameter (model B), leading to the GNF for $\alpha < 0$, and HU for $\alpha > 0$. We summarize those results in Fig. 3.

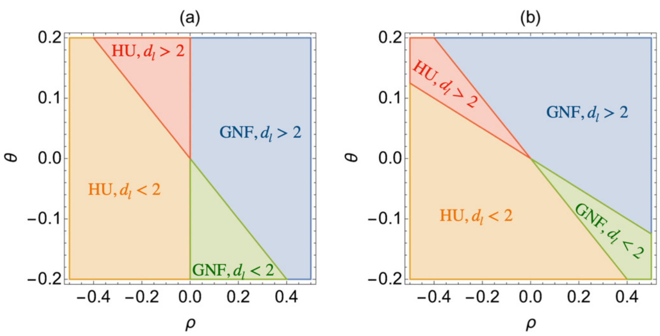

FIG. 3. Phase behaviors for the model A (a) and model B (b).

B. Hyperuniformity, giant number fluctuation, and lower critical dimension

Our first expectation was that the HU would decrease d_l from the equilibrium value $d_l^{\rm eq} = 2$, and the GNF would increase d_l. This expectation is correct for the spatiotemporally positive correlated noise ($\rho > 0, \theta > 0$) and anticorrelated noise ($\rho < 0, \theta < 0$), see Fig. 3. However, for the intermediate cases, $\rho < 0, \theta > 0$ and $\rho > 0, \theta < 0$, the HU or GNF does not always guaranty $d_l < 2$ or $d_l > 2$, see Fig. 3. Further studies would be beneficial to elucidate the relation between the HU, GNF, and d_l.

C. Perspective on temporally correlated noise

The temporally correlated noise for $-1/2 < \theta < 1/2$ has been studied extensively in the context of the anomalous diffusion in crowded environments, because a free particle driven by the noise $\dot{x} = \xi$ exhibits the subdiffusion $\langle x(t)^2\rangle \sim t^{1+2\theta}$ for $-1/2 < \theta < 0$ and superdiffusion for $0 < \theta < 1/2$, see Refs. [27,44] for reviews. However, relatively few studies have been done on the effects of the temporal correlation on critical phenomena. For example, in Refs. [38,45,46], the authors studied the effect of exponentially correlated noise on the φ^4 model and found the same universality as the equilibrium Ising model. In Ref. [47], the authors studied the O(n) model with the power-law correlated noise, but the noise was introduced in a way that preserves the detailed balance. Thus, the critical dimensions and the static critical exponents are unchanged from those in equilibrium. On the contrary, nonequilibrium noises, such as the $1/f$ noises, often show the power-law frequency dependence of the power spectrum, naturally leading to the long-range temporal correlation [28,48–51]. Our research has demonstrated the emergence of novel phenomena, such as the GNF, HU, and new universality classes in systems driven by such long-range temporally correlated noise. We hope that our findings will motivate further investigation into the fascinating properties of these systems.

D. Systems driven by imperfect periodic or quasiperiodic forces

Tissues are often driven by periodic deformation of cells [52]. In chiral active matter, constituent particles spontaneously rotate due to asymmetry of the driving forces [25,53]. The driving force of those systems would be approximated by temporally periodic functions. In previous work, we investigated a model driven by temporally periodic but spatially uncorrelated driving forces and found that the model exhibits the HU and smaller value of the lower critical dimension than that in equilibrium $d_l < 2$ [26]. However, the completely periodic function does not exist in reality due to friction or other uncontrollable effects. The effects of the imperfection of periodic patterns have been investigated extensively in the context of the HU, and it is known that the Fourier spectrum often exhibits the power law with a positive exponent in these cases [34,54]. For the simplest example, we consider an imperfect periodic pulse [34]:

$$\xi(t) = \lim_{T\to\infty}\sum_{n=1}^{T}\delta(t - na - \eta_n), \tag{63}$$

where η_n represents a perturbation to a periodic pulse. For simplicity, let us assume that η_n is an independent and identically distributed Gaussian random variable of zero mean and variance σ. Then, the power spectrum of $\xi(t)$ can be calculated as follows [34]:

$$D(\omega) = \lim_{T\to\infty}\frac{1}{T}\overline{\left|\sum_{n=1}^{T} e^{i\omega(na+\eta_n)}\right|^2}$$
$$= 1 + e^{-\sigma\omega^2}(D_0(\omega) - 1), \tag{64}$$

where the overline denotes the average for η_n, and $D_0(\omega)$ represents the spectrum of the periodic pulse:

$$D_0(\omega) = \lim_{T\to\infty}\frac{1}{T}\left|\sum_{n=1}^{T} e^{i\omega na}\right|^2. \tag{65}$$

$D_0(\omega)$ is nothing but the static structure factor of a one-dimensional lattice, and in particular $D_0(\omega) = 0$ for sufficiently small ω [34]. For $\omega \ll 1$, we get

$$D(\omega) \sim 1 - e^{-\sigma\omega^2} \sim \sigma\omega^{-2\theta} \tag{66}$$

with $\theta = -1$. This simple example demonstrated that the power-law spectrum with negative θ can naturally arise due to the imperfection of the periodic pattern. More systematic studies for various types of imperfections have been investigated in Ref. [34]. The similar power law of the Fourier spectrum has been also reported for one-dimensional quasiperiodic sequences [54,55]. Do systems driven by imperfect periodic or quasiperiodic forces exhibit the HU and symmetry breaking transition in $d \leqslant 2$, as predicted by our theory? Further theoretical and numerical studies would be beneficial to elucidate this point.

ACKNOWLEDGMENTS

We thank K. Miyazaki and A. Ikeda for useful discussions. This project has received JSPS KAKENHI Grants No. 21K20355 and No. 23K13031.

APPENDIX: SCALING OF μ

To determine μ, one should solve the following self-consistent equation:

$$1 = TG(\mu) \equiv TA\int_0^{q_D} dq\,\frac{q^{d-1+m}}{(q^2+\mu)^n}, \tag{A1}$$

where A, n, and m are constants. We want to derive the scaling behavior of μ near the critical point:

$$T_c = \left[A\int_0^{q_D} dq q^{d-1+m-2n}\right]^{-1}. \tag{A2}$$

For $d+m-2n>0$, the denominator of Eq. (A2) diverges, and thus the model does not have the critical point at finite T. This implies that the lower critical dimension is

$$d_l = 2n - m. \tag{A3}$$

When $d > 2n-m+2$, $G(\mu)$ can be expanded as

$$\frac{1}{T} = G(0) + \mu G'(0) + \cdots$$
$$= \frac{1}{T_c} + \mu G'(0) + \cdots, \tag{A4}$$

leading to

$$\mu \sim (T - T_c)^1. \tag{A5}$$

On the contrary, if $d \in (2n-m, 2n-m+2)$, $G'(\mu)$ for small μ behaves as

$$G'(\mu) \sim \mu^{\frac{d+m-(2n+2)}{2}}, \tag{A6}$$

implying

$$G(\mu) - G(0) = \int_0^{\mu} d\mu' G'(\mu') \sim \mu^{\frac{d+m-2n}{2}}, \tag{A7}$$

leading to

$$\frac{1}{T} = G(\mu) = \frac{1}{T_c} - B\mu^{\frac{d+m-2n}{2}}, \tag{A8}$$

where B is a constant. Therefore, the scaling of μ for $\mu \ll 1$ is

$$\mu \sim (T-T_c)^{\frac{2}{d+m-2n}} \sim (T-T_c)^{\frac{2}{d-d_l}}. \tag{A9}$$

The above results imply that the upper critical dimension is

$$d_u = 2n - m + 2 = d_l + 2. \tag{A10}$$

[1] H. Nishimori and G. Ortiz, *Elements of Phase Transitions and Critical Phenomena* (Oxford University Press, Oxford, 2010).
[2] Y. Imry and S.-k. Ma, Phys. Rev. Lett. **35**, 1399 (1975).
[3] M. Schwartz, J. Villain, Y. Shapir, and T. Nattermann, Phys. Rev. B **48**, 3095 (1993).
[4] W. Janke and R. Villanova, Phys. Lett. A **209**, 179 (1995).
[5] H. Barghathi and T. Vojta, Phys. Rev. Lett. **113**, 120602 (2014).
[6] J. Luck, J. Phys. A: Math. Gen. **20**, 1259 (1987).
[7] C. Sire, Int. J. Mod. Phys. B **07**, 1551 (1993).
[8] N. D. Mermin and H. Wagner, Phys. Rev. Lett. **17**, 1133 (1966).
[9] K. E. Bassler and Z. Rácz, Phys. Rev. E **52**, R9 (1995).
[10] M. D. Reichl, C. I. Del Genio, and K. E. Bassler, Phys. Rev. E **82**, 040102 (2010).
[11] F. Corberi, E. Lippiello, and M. Zannetti, Phys. Rev. E **65**, 046136 (2002).
[12] H. Nakano, Y. Minami, and S.-i. Sasa, Phys. Rev. Lett. **126**, 160604 (2021).
[13] T. Vicsek, A. Czirók, E. Ben-Jacob, I. Cohen, and O. Shochet, Phys. Rev. Lett. **75**, 1226 (1995).
[14] J. Toner and Y. Tu, Phys. Rev. Lett. **75**, 4326 (1995).
[15] S. A. M. Loos, S. H. L. Klapp, and T. Martynec, Phys. Rev. Lett. **130**, 198301 (2023).
[16] L. P. Dadhichi, J. Kethapelli, R. Chajwa, S. Ramaswamy, and A. Maitra, Phys. Rev. E **101**, 052601 (2020).
[17] S. Torquato, Phys. Rep. **745**, 1 (2018).
[18] L. Galliano, M. E. Cates, and L. Berthier, Phys. Rev. Lett. **131**, 047101 (2023).
[19] P. A. Crossley, L. M. Schwartz, and J. R. Banavar, Appl. Phys. Lett. **59**, 3553 (1991).
[20] J. H. Weijs, R. Jeanneret, R. Dreyfus, and D. Bartolo, Phys. Rev. Lett. **115**, 108301 (2015).
[21] M. Huang, W. Hu, S. Yang, Q.-X. Liu, and H. Zhang, Proc. Natl. Acad. Sci. USA **118**, e2100493118 (2021).
[22] B. Zhang and A. Snezhko, Phys. Rev. Lett. **128**, 218002 (2022).
[23] D. Hexner and D. Levine, Phys. Rev. Lett. **118**, 020601 (2017).
[24] Q.-L. Lei and R. Ni, Proc. Natl. Acad. Sci. USA **116**, 22983 (2019).
[25] Y. Kuroda and K. Miyazaki, J. Stat. Mech. (2023) 103203.
[26] H. Ikeda and Y. Kuroda, arXiv:2304.14235.
[27] J.-P. Bouchaud and A. Georges, Phys. Rep. **195**, 127 (1990).
[28] I. Eliazar and J. Klafter, Proc. Natl. Acad. Sci. USA **106**, 12251 (2009).
[29] P. M. Chaikin, T. C. Lubensky, and T. A. Witten, *Principles of Condensed Matter Physics*, Vol. 10 (Cambridge University Press, Cambridge, UK, 1995).
[30] E. Medina, T. Hwa, M. Kardar, and Y.-C. Zhang, Phys. Rev. A **39**, 3053 (1989).
[31] H. Janssen, U. C. Täuber, and E. Frey, Eur. Phys. J. B **9**, 491 (1999).
[32] E. Katzav and M. Schwartz, Phys. Rev. E **70**, 011601 (2004).
[33] D. Squizzato and L. Canet, Phys. Rev. E **100**, 062143 (2019).
[34] J. Kim and S. Torquato, Phys. Rev. B **97**, 054105 (2018).
[35] R. Zwanzig, *Nonequilibrium Statistical Mechanics* (Oxford University Press, Oxford, 2001).
[36] To satisfy the detailed balance, the left-hand side of Eq. (3) should be replaced as

$$\frac{\partial \phi_a(\boldsymbol{x},t)}{\partial t} \to \int_{-\infty}^{t} dt' \int d\boldsymbol{x}' D(t-t', \boldsymbol{x}-\boldsymbol{x}') \frac{\partial \phi_a(\boldsymbol{x}',t')}{\partial t'}, \tag{A11}$$

i.e., one should consider the (overdamped) generalized Langevin equation [35,47].
[37] T. Nattermann, in *Spin Glasses and Random Fields* (World Scientific, Singapore, 1998), pp. 277–298.
[38] C. Maggi, N. Gnan, M. Paoluzzi, E. Zaccarelli, and A. Crisanti, Commun. Phys. **5**, 55 (2022).
[39] M. Henkel and M. Pleimling, *Non-Equilibrium Phase Transitions Volume 2: Ageing and Dynamical Scaling Far from Equilibrium*, Theoretical and Mathematical Physics (Springer, Dordrecht, 2010).
[40] T. H. Berlin and M. Kac, Phys. Rev. **86**, 821 (1952).
[41] M. Kac and C. J. Thompson, J. Math. Phys. **18**, 1650 (1977).

[42] V. Narayan, S. Ramaswamy, and N. Menon, Science **317**, 105 (2007).
[43] A. Onuki, *Phase Transition Dynamics* (Cambridge University Press, Cambridge, UK, 2002).
[44] F. Höfling and T. Franosch, Rep. Prog. Phys. **76**, 046602 (2013).
[45] J. García-Ojalvo and J. M. Sancho, Phys. Rev. E **49**, 2769 (1994).
[46] J. Sancho, J. Garcia-Ojalvo, and H. Guo, Physica D **113**, 331 (1998).
[47] J. Bonart, L. F. Cugliandolo, and A. Gambassi, J. Stat. Mech.: Theory Exp. (2012) P01014.
[48] R. F. Voss and J. Clarke, Phys. Rev. B **13**, 556 (1976).
[49] P. Bak, C. Tang, and K. Wiesenfeld, Phys. Rev. Lett. **59**, 381 (1987).
[50] P. Dutta and P. M. Horn, Rev. Mod. Phys. **53**, 497 (1981).
[51] E. Milotti, arXiv:physics/0204033.
[52] Y. Zhang and É. Fodor, Phys. Rev. Lett. **131**, 238302 (2023).
[53] B. Liebchen and D. Levis, Europhys. Lett. **139**, 67001 (2022).
[54] E. Oğuz, J. E. Socolar, P. J. Steinhardt, and S. Torquato, Acta. Crystallogr. A: Found Adv. **75**, 3 (2019).
[55] E. C. Oğuz, J. E. S. Socolar, P. J. Steinhardt, and S. Torquato, Phys. Rev. B **95**, 054119 (2017).